

# Tilted-Chain Lamellar Morphology in Initially Crystallized Low Molecular Weight Poly(ethylene oxide) from Raman Longitudinal Acoustic Mode Spectra

Insun Kim and Samuel Krimm\*

Macromolecular Science & Engineering Center and  
Department of Physics, University of Michigan,  
Ann Arbor, Michigan 48109

Received June 1, 1994

The concept of integer fold (IF) structures in poly(ethylene oxide) (PEO) was based on observations of stepwise increases in small-angle X-ray scattering (SAXS) lamellar spacings in low molecular weight fractions as a function of crystallization temperature<sup>1</sup> and annealing temperature.<sup>2</sup> This was supported by Raman longitudinal acoustic mode (LAM) observations<sup>3</sup> which, together with transmission electron microscope studies,<sup>4</sup> implied that the chain ends were at the lamellar surface and the chain axes were perpendicular to this surface. Similar IF structures were shown to be present in the final stages of crystallization of ultralong *n*-paraffins.<sup>5</sup>

A noninteger from (NIF) of crystalline PEO was first seen in LAM studies of low molecular weight PEO<sup>6</sup> and was subsequently shown by LAM<sup>7</sup> and SAXS<sup>8</sup> studies to be associated with the early stages of crystallization, transforming with time to IF structures. Similar behavior had been observed earlier for the ultralong *n*-paraffins by time-lapse synchrotron SAXS studies.<sup>9</sup> Although tilted-chain forms were found in this case for the extended (E) and folded (F2, for once-folded, etc.) structures, nothing could be said about the NIF structures since the X-ray lamellar spacings were not accompanied by comparable LAM measurements.

We have obtained time-resolved LAM spectra of PEO as a function of crystallization temperature ( $T_c$ ),<sup>10</sup> which, together with SAXS measurements on the same material crystallized in the same way,<sup>8,11</sup> show that NIF structures in the early stages of crystallization are comprised of chains inclined to the lamellar surface. On conversion to the E or F2 forms, the chain axis becomes perpendicular to the lamellar surface.

Before discussing the results, it is useful to recall the differences between the kinds of information provided by LAM and SAXS measurements. The LAM of PEO measures the helix axial stem length,  $L_L$ , in the crystalline lattice.<sup>12</sup> Its frequency,  $\nu_L$ , is particularly sensitive to interchain interactions<sup>12</sup> and is not much affected by the presence of a fold at the end of the stem.<sup>13</sup> Normal-mode analyses<sup>12</sup> and measured LAM frequencies of a range of oligomers<sup>7</sup> provide the basis for converting  $\nu_L$  into  $L_L$ . The SAXS measurement gives the interlamellar spacing,  $L_S$ , which consists of the crystalline lamellar thickness plus that of the interlamellar layer,  $L_A$ . It is clear that  $L_L \geq L_S - L_A$ , where the equality applies to chain axes perpendicular to the lamellar surface and the inequality holds for tilted chains.

The PEO 3000 that we used was kindly provided by Professor S. Z. D. Cheng and was identical to that used in the X-ray studies.<sup>8,11</sup> Its  $\bar{M}_n$  of 2990 ( $\bar{M}_w/\bar{M}_n = 1.02$ ) implies an average extended helix length of  $\bar{L}_M(E) = 189$  Å.<sup>14</sup> The LAM spectrum at room temperature of a well-crystallized sample ( $T_c = 47$  °C,  $t_c = 5$  days) is shown in Figure 1. The  $\nu_L = 5.7$  cm<sup>-1</sup> band corresponds to  $L_L = 196$  Å, i.e., to E chains, which together with  $L_S = 196$  Å<sup>11</sup> indicates that the chains are perpendicular to the lamellar surface. The  $\nu_L = 12.4$  cm<sup>-1</sup> band corresponds to  $L_L = 95$

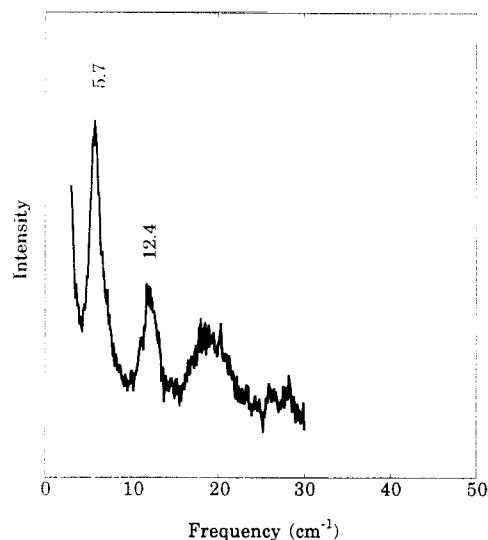


**Figure 1.** Low-frequency Raman spectrum of PEO 3000. The sample was crystallized at 47 °C for 5 days and the spectrum taken at room temperature.

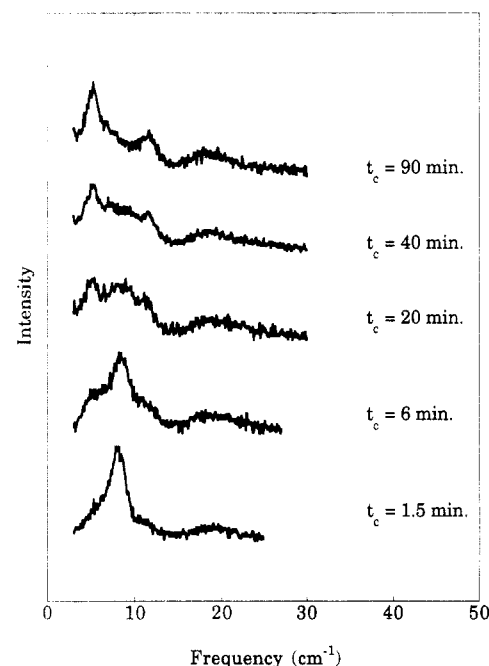


**Figure 2.** Low-frequency Raman spectra of PEO 3000 during crystallization at 38.5 °C.

Å, and since  $\bar{L}_M(F2) = 90$  Å (allowing for three monomer units in the fold<sup>7,13</sup>), this band is clearly associated with F2 chains, also seen in SAXS by the presence of an intense peak at  $L_S = 105$  Å.<sup>11</sup> This implies the existence of what we have called F2 monolayer, F2(M), lamellae,<sup>7</sup> which again are consistent with perpendicularly oriented chains. (Incidentally, if the values are correct, the difference between  $L_L$  and  $L_S$  would indicate an interlamellar layer of  $L_A \approx 10$ – $15$  Å.) The 19.5 cm<sup>-1</sup> band is a lattice mode,<sup>7</sup> and its presence in the spectrum is an indication of the presence of the standard crystalline lattice.<sup>14</sup>

In Figure 2 we show the LAM spectra of a sample crystallized at  $T_c = 38.5$  °C as a function of time (the collection time for each spectrum was about 3 min). The initial ( $t_c = 1.5$  min) LAM band appears at  $\nu_L = 8.0$  cm<sup>-1</sup>, which, after correcting for the temperature difference (by obtaining spectra of the well-crystallized sample of Figure 1 at 38.5 °C), corresponds to  $L_L = 139$  Å. It is important to note the presence of the lattice mode at 19.5 cm<sup>-1</sup>,

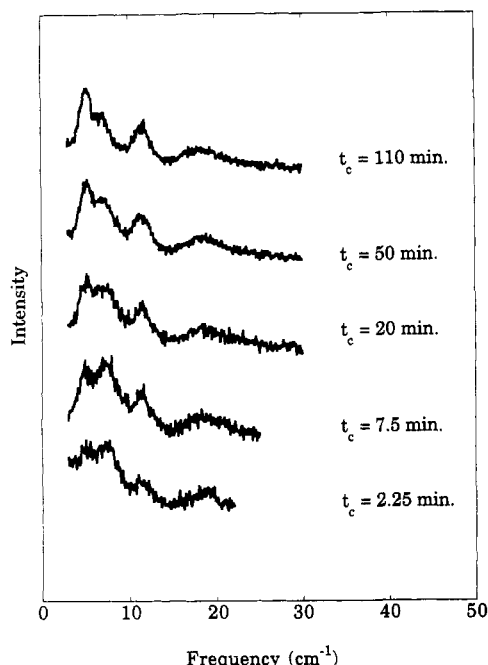


**Figure 3.** Low-frequency Raman spectra of PEO 3000 during crystallization at 42.5 °C.

indicating that this obviously NIF structure occurs in the usual crystalline lattice<sup>14</sup> and therefore the stem lengths can be determined in the standard way from the calibration curve.<sup>7</sup> (Wide-angle X-ray diffraction<sup>15</sup> also confirms the initial presence of the usual crystal lattice.<sup>14</sup>) X-ray results<sup>8,11</sup> give the initial  $L_S = 126$  Å, which together with  $L_L = 139$  Å indicates that the chains are tilted with respect to the perpendicular orientation, with a minimum tilt angle of 25.0°. This is similar to the value of 26° found for solution-grown single crystals.<sup>16</sup> (Note that, if there is thermal lag in its interior while the sample is being brought to  $T_c$ , the larger SAXS vs LAM sample size, viz., 20–30 mg<sup>11</sup> vs 2–3 mg,<sup>10</sup> would result in more crystallization at higher temperature occurring in the SAXS experiment, with consequent weighting toward larger  $L_S$  values. Thus, in this case the comparable  $L_S$  would be <126 Å, and the tilt angle would be larger. Of course, the crystalline portion of the lamella may also be smaller because of  $L_A$ .) With increasing  $t_c$ , the NIF band decreases in intensity (while remaining at the same  $\nu_L$ ) and new bands grow in at positions of the E and F2 structures until these dominate by  $t_c = 90$  min. Some NIF structure still persists at  $t_c = 60$  min, although this is not evident in the SAXS curve.<sup>8,11</sup>

When  $T_c$  is raised to 42.5 °C (Figure 3), the initial LAM spectrum has an observed  $\nu_L(\text{NIF}) = 7.4$  cm<sup>-1</sup>, corresponding (after temperature correction) to  $L_L(\text{NIF}) = 149$  Å, and the  $\nu_L(\text{E})$  and  $\nu_L(\text{F2})$  bands make their appearance relatively sooner. The SAXS results give  $L_S(\text{NIF}) = 130$  Å, implying a minimum tilt angle of 29.4°, but whereas the SAXS NIF peak is essentially gone by  $t_c = 70$  min,<sup>11</sup> we still see evidence of  $\nu_L(\text{NIF})$  at  $t_c = 110$  min.

We have also examined methoxylated PEO (MPEO), and our  $L_L$  results, together with the comparable  $L_S$  values,<sup>17</sup> are given in Table 1, as well as the PEO results. As for PEO, the initial  $L_L$  for MPEO, also indicative of NIF structure, is larger than the comparable  $L_S$ , leading to the conclusion that these chains are also tilted.

These results show several important features. (1) The initial NIF band is well-defined, having a half-width comparable to those for the E and F2 chains. This indicates that the initial NIF stem-length distribution is related to a relatively specific structure and would seem

**Table 1. Raman LAM Chain Lengths ( $L_L$ ) and SAXS Lamellar Periodicities ( $L_S$ ) Observed at the Beginning of Crystallization for PEO 3000 and MPEO 3000<sup>a</sup>**

PEO 3000				MPEO 3000 <sup>a</sup>			
$T_c$ (°C)	$L_L$ (Å)	$L_S$ (Å) <sup>b</sup>	$\theta$ (deg) <sup>c</sup>	$T_c$ (°C)	$L_L$ (Å)	$L_S$ (Å) <sup>b</sup>	$\theta$ (deg) <sup>c</sup>
38.5	139	126	25.0	39.0	146	138	19.1
42.5	149	130	29.3	43.0	155	140	25.4
				47.0	159	148	21.4

<sup>a</sup> MPEO 3000 represents  $\alpha,\omega$ -methoxylated PEO with  $\bar{M}_n = 3050$  and  $\bar{M}_w/\bar{M}_n = 1.02$ . <sup>b</sup> For PEO 3000,  $L_S$  was measured at  $T_c = 38.4$  and 42.4 °C, respectively;<sup>11</sup> for MPEO 3000, 47.1 °C was used.<sup>17</sup> <sup>c</sup>  $\theta$  represents the chain tilt angle from the perpendicular to the lamellar surface (for which  $\theta = 0^\circ$ ).

to eliminate models with substantial stem-length variability.<sup>11</sup> (2) The clear evidence that  $L_L > L_S$  shows that the PEO helix axes are inclined from the perpendicular to the lamellar surfaces. This could arise from a tilt of chains within a fold plane, a stagger between fold planes, or both. (3) The position of  $\nu_L(\text{NIF})$  remains constant with  $t_c$ , although the band tends to broaden (at least at lower  $T_c$ ) as it diminishes in intensity and the E and F2 structures develop. This would seem to indicate the absence of stable intermediate structures. (4) With increasing  $T_c$ , two effects are seen:  $L_L$  for the NIF structure increases, also seen for this  $\bar{M}_n$  in SAXS,<sup>15</sup> and the conversion of NIF to E and F2 structures occurs more rapidly. Both of these characteristics are consistent with a kinetic driving mechanism for the initial crystallization.

The origin of the tilted-chain NIF morphology is not clear at present, but we note one factor that may be involved. If chain folding is associated with the NIF structure and such folding occurs in the (120) planes,<sup>18</sup> then the crystal structure<sup>14</sup> requires that adjacent stems have opposite helical chirality. If a molecule initially crystallizing from the melt has only a single chirality and if this is maintained in the folded state in the crystal, it would be expected that the (120) fold would have a structure different from that when chirality reversal occurs. Similarly, if folding occurred in the (100) planes, which does not require chirality reversal but would demand traversal of a larger stem-to-stem separation, the fold structure would be different. In either case, the fold could lead to chain stagger within a fold plane or stagger between planes, resulting in a tilted-chain lamellar morphology. Reorganization in the solid state into the more stable E and F2 structures (given that the lamellae are not surrounded by the melt as in the case of thickening of single crystals<sup>19</sup>) would then be associated with the necessary chirality reversals as well as a possible change in the fold plane. While obviously speculative at this point, such mechanisms deserve examination as possible components of tilted-chain NIF structure and transformation.

**Acknowledgment.** This research was supported by NSF Grant DMR-9110353.

## References and Notes

- (1) Arlie, J. P.; Spegt, P.; Skoulios, A. *Makromol. Chem.* **1967**, *104*, 212.
- (2) Spegt, P. *Makromol. Chem.* **1970**, *139*, 139.
- (3) Hartley, A.; Leung, Y. K.; Booth, C.; Sheppard, I. W. *Polymer* **1976**, *17*, 354.
- (4) Cheng, S. Z. D.; Bu, H. S.; Wunderlich, B. *Polymer* **1988**, *29*, 579.
- (5) Ungar, G.; Stejny, J.; Keller, A.; Bidd, I.; Whiting, M. C. *Science* **1985**, *229*, 386.
- (6) Song, K.; Krimm, S. *Macromolecules* **1989**, *22*, 1504.

- (7) Song, K.; Krimm, S. *Macromolecules* **1990**, *23*, 1946.
- (8) Cheng, S. Z. D.; Zhang, A.; Chen, J. *J. Polym. Sci., Part C: Polym. Lett.* **1990**, *28*, 233.
- (9) Ungar, G.; Keller, A. *Polymer* **1986**, *27*, 1835.
- (10) Kim, I.; Krimm, S., unpublished results.
- (11) Cheng, S. Z. D.; Zhang, A.; Chen, J.; Heberer, D. P. *J. Polym. Sci., Part B: Polym. Phys.* **1991**, *29*, 287.
- (12) Song, K.; Krimm, S. *J. Polym. Sci., Part B: Polym. Phys.* **1990**, *28*, 35.
- (13) Song, K.; Krimm, S. *J. Polym. Sci., Part B: Polym. Phys.* **1990**, *28*, 63.
- (14) Takahashi, Y.; Tadokoro, H. *Macromolecules* **1973**, *6*, 672.
- (15) Cheng, S. Z. D.; Wu, S. S.; Chen, J.; Zhuo, Q.; Quirk, R. P.; von Meerwall, E. D.; Hsiao, B. S.; Habenschuss, A.; Zschack, P. R. *Macromolecules* **1993**, *26*, 5105.
- (16) Baltá Calleja, F. J.; Hay, I. L.; Keller, A. *Kolloid Z. Z. Polym.* **1966**, *209*, 128.
- (17) Cheng, S. Z. D.; Chen, J.; Zhang, Z.; Heberer, D. P. *J. Polym. Sci., Part B: Polym. Phys.* **1991**, *29*, 299.
- (18) Lotz, B.; Kovacs, A. J.; Bassett, G. A.; Keller, A. *Kolloid Z. Z. Polym.* **1966**, *209*, 115.
- (19) Kovacs, A. J.; Straupe, C. *Discuss. Faraday Soc.* **1979**, *68*, 225.